Coupled Systems Mechanics, *Vol. 14, No. 2 (2025) 105-127*
https://doi.org/10.12989/csm.2025.14.2.105

Vibration investigation of an imperfect FGM cylindrical shell reinforced by various types of stiffeners with temperature-dependent properties resting on an elastic foundation

Ahmed Muthanna[1], Mohammed Ali[2], Hamad M. Hasan[1], Khalid B. Najim[3], Emad Kadum Njim[*4], Royal Madan[**5] and Mohammed H. Al-Maamori[6]

[1]*Department of Mechanical Engineering, College of Engineering, University of Anbar¸ Ramadi, Iraq*
[2]*Department of Medical Instruments Engineering Techniques, College of Engineering, University of Al Maarif, Al Anbar,31001, Iraq*
[3]*Department of Civil Engineering, College of Engineering, University of Anbar, Ramadi, Iraq*
[4]*Ministry of Industry and Minerals, State Company for Rubber and Tires Industries, Iraq*
[5]*Department of Mechanical Engineering, Graphic Era (Deemed to be University), Dehradun 248002, Uttarakhand, India*
[6]*Prosthetics and Orthotics Engineering Department, College of Engineering, AL-Mustaqbal University, 51001, Babylon, Iraq*

(Received February 12, 2025, Revised March 24, 2025, Accepted April 11, 2025)

Abstract. This study examines the vibration response of imperfect functionally graded (FG) cylindrical shells reinforced with different types of eccentrically placed stiffeners. The material composition follows a power-law distribution, varying with different grading indices. The analysis is conducted analytically under simply supported boundary conditions, considering longitudinal and transverse stiffeners of circular, rectangular, and triangular cross-sections. The cylindrical shell, resting on an elastic foundation, is subjected to thermo-mechanical loading. The governing equations are derived using the first-order shear deformation theory, incorporating von Kármán-Donnell nonlinear geometric formulation and the smeared stiffener method. A numerical approach combining the fourth-order Runge-Kutta method and Galerkin's procedure is employed to evaluate the dynamic response and natural frequencies. Results reveal that increasing foundation stiffness enhances natural frequencies by 15% and reduces vibration amplitude. Conversely, elevated temperature leads to a 12% reduction in natural frequencies and a decrease in structural rigidity, highlighting the coupled effects of thermal and mechanical loads on the shell's dynamic behavior.

Keywords: first-order shear deformation theory; functionally graded material (FGM); nonlinear vibration; smeared stiffeners method (SSM)

1. Introduction

∗Corresponding author, Ph.D., E-mail: emad-njim@scrit.gov.iq
∗∗Co-corresponding author, Ph.D., E-mail: royalmadan.me@geu.ac.in

Copyright © 2025 Techno-Press, Ltd.
http://www.techno-press.org/?journal=csm&subpage=8 ISSN: 2234-2184 (Print), 2234-2192 (Online)

Cylindrical structures are often used in various fields of engineering like mechanical, civil, chemical, aerospace, and electrical applications (Daneshmand *et al*. 2023, Kadum Njim *et al.* 2024). With advancing the use of these kinds of structures in different engineering places such as gasoline engines, defense productions, chemical pipelines, aerospace structures, power plants, aircraft engines, and fusion reactors, the behavior of these structures should be examined to keep normal operation without the failure of these structures (Madan *et al.* 2024, Zohra *et al*. 2024, Zouatnia *et al*. 2024, Mahendra *et al*. 2023). Panels are reinforced by stiffeners, which are made of advanced materials called functionally graded materials (FGM) and are widely applied in different kinds of engineering applications such as aircraft, ship hulls, buildings, and bridges. From the literature, it was found that the elastic foundation has a significant impact on the vibration amplitude and natural frequencies. Also, apart from the thermo-mechanical loading, it would be interesting to analyze the effect of temperature-dependent material properties on dynamic characteristics (Madan *et al*. 2023, Singh *et al*. 2024). The presence of imperfections and different types of stiffeners necessitates a detailed investigation to enhance performance, stability, and durability.

Free vibration analysis of stiffened laminated plates was studied using finite element method (FEM) (Singh Rajawat *et al.* 2018). An analytical approach to study the free vibration of three-layer cylindrical shells with FG in the middle layer was studied (Li *et al*. 2010). Furthermore, an analytical method to study the stability of FGM cylindrical panels influenced by axial compression was carried out. They displayed that any increase in the value of the volume fraction index leads to a decrease in the magnitude of buckling and post-buckling (Duc and Tung 2010). A 3D vibration analysis of layered FG cylindrical sandwich shells was performed analytically (Arefi *et al*. 2016). The most important result they obtained was in decrease in frequency when the index of non-homogeneous (FGP) layers increases, while the frequency rises significantly when the ratio of the thickness of the middle layer to the length of the cylindrical increases. Employed first-order shear deformation theory to study the behavior of vibration of (FGM) truncated conical shells surrounded by Winkler and Pasternak foundation. The shear strains lead to a reduction of the value of the frequency parameters from 2.71% to 0.58% (Deniz *et al.* 2016). In (Sofiyev 2018), studied the distribution of composite materials in various directions on free vibration of layered orthotropic conical shells. This means using FSDT leads to a decrease in the influence of the number of layers on the fundamental frequency parameter values. The dynamic stability of functionally graded orthotropic cylindrical shell envelopes resting on an elastic foundation under a linearly increasing load, with the influence of damping, was investigated by (Gao *et al.* 2018). Further, employed the third-order shear deformation theory to analyze the free vibration of 2D-FGM beam under different boundary conditions (Karamanlı 2018). They found that increasing the gradient index in the direction of the thickness leads to a reduction in natural frequencies of clamped-clamped 2D-FGB.

To examine the buckling stresses and natural frequencies for the shallow shell structure formed of a new material which is FGM while taking into account the influences of rotatory inertia, and normal transverse shear deformations. The mechanical properties are assumed to change according to (P-FGM). Three kinds of simply supported shells (negative, zero, and positive) were analyzed. When the range of power index is between 0 to 10, the buckling stresses and natural frequencies decrease rapidly (Matsunaga 2008). A problem of thermal buckling of FG porous rectangular plate using Navier's method was solved and the influence of critical buckling temperature was investigated (Ellali *et al*. 2024). A semi-analytical solution to study the bending that occurs in the rotating disks formed of the functionally graded material (FGM) under different boundary

conditions. They explained the stresses in a state of the disk manufactured of the homogeneous material (full-metal and full-ceramics) were higher than stresses in a state of the disk manufactured of FGM (Bayat *et al.* 2009). Developed an improved theoretical model for interfacial shear stress analysis in composite beams with an aluminum-sandwich honeycomb core, incorporating adherend shear deformations and providing accurate stress distributions for diverse composite structures (Tayeb *et al*. 2024). The study analyzes a micro-elongated thermoelastic thick circular plate under thermomechanical sources, solving via Laplace-Hankel transforms. Results highlight micro-elongation effects, stress-temperature behavior, and deformation insights for advanced structural materials (Kumar *et al*. 2024). A non-linear vibration analysis of imperfect ES-FGM thick shallow shells resting on the elastic foundation was carried out analytically by (Huy Bich *et al.* 2014). A first-order shear deformation theory (FSDT) was employed to study the nonlinear dynamic response of imperfect (ES-FGM) thick circular cylindrical shells neglecting Volmir's assumptions (Duc and Thang 2015).

A nonlinear dynamical analysis of layered reinforced shallow shells was performed. The response of nonlinear dynamical analysis was determined by utilizing an iterative method in connection with the Newmark continuous acceleration sketch exposed to the excitation force. They displayed that the stiffeners reduce the amplitude of the midpoint deflection and the influence of geometric nonlinear was complicated (Bich and Long 2007). The nonlinear vibration response of functionally graded thick plates under thermal stress, supported by an elastic foundation, was analyzed using the third-order shear deformation plate theory (Duc *et al*. 2016), which found that the foundation helps reduce vibration amplitude in a thermal environment. A non-linear dynamic analysis of eccentrically stiffened functionally graded material (ES-FGM) cylindrical panels was performed by (Bich *et al*. 2012). The effect of porosity on functionally graded cylindrical panels was investigated using classical shell theory (Mouthanna *et al.* 2023) resting on a Pasternak elastic foundation, focusing on the effects of thermo-humidity conditions was studied (Kiarasi *et al.* 2022). The effect of porosity on a crack FG plate has been performed analytically under various boundary conditions (Khayra *et al*. 2024, Neamah *et al*. 2025). Furthermore, the vibration response of sandwich structures under varying boundary conditions, geometrical and material parameters with and without porosity effects was performed analytically (Kadum Njim *et al*. 2024, Njim *et al*. 2024, Raad *et al*. 2024). A nonlinear drill string model for inclined well drilling was developed and analyzed the effects of mudflow, weight on the bit, and damping. Findings show that higher mud flow reduces vibrations, while increased weight lowers natural frequencies but amplifies vibrations (Taheran *et al.* 2016). Furthermore, investigates 2-mm Al/Cu bimetallic laminates produced via asymmetric roll bonding (RB) with varying thickness reductions and mismatch rolling speeds. Finite element simulations and experiments analyzed bond strength, revealing optimal bonding at a 1:1.2 rolling speed ratio (Vini and Daneshmand 2019).

The present study aims to investigate the influence of numerous stiffener geometric shapes on the nonlinear natural frequencies of eccentrically stiffened functionally graded material (ES-P-FGM) cylindrical panels under a thermal environment with Winkler and Pasternak foundations. The governing equations of motion are formulated using the first-order shear deformation theory (FSDT). To analyze the dynamic behavior of functionally graded material (FGM) cylindrical panels, the fourth-order Runge-Kutta numerical method is employed, enabling the evaluation of nonlinear dynamic responses and natural frequencies. This study explores the effects of various parameters, including the volume fraction index, geometric properties, the presence of stiffeners, temperature variations, and the influence of elastic foundations, on the nonlinear dynamic response of FGM cylindrical panels.

(a) cylindrical panel with circular stiffeners

(b) cylindrical panel with rectangle stiffeners

(c) cylindrical panel with triangle stiffeners

Fig. 1 The stiffened cylindrical panel on the elastic foundations in the thermal environment (a) Circular stiffeners (b) Rectangle stiffeners (c) Triangle stiffeners

2. FGM cylindrical panels on elastic foundation formulation

This study considers functionally graded material composed of a blend of metal and ceramic, with their volume fractions determined by a power-law distribution (P-FGM)

$$V_m + V_c = 1, \qquad V_c = V_c(z) = \left(\frac{2z+h}{2h}\right)^N, \tag{1}$$

where (N) represents the volume fraction index. The subscripts (c) and (m) define the composition of metal and ceramic. As per power law, the Young modulus (E), density (ρ) and the thermal expansion (α) can be illustrated in the form below (Ali and Hasan 2019, Ali and Hasan 2022)

$$\begin{aligned} E(z) &= E_m V_m + E_c V_c = E_m + (E_c - E_m)\left(\frac{2z+h}{2h}\right)^N, \\ \rho(z) &= \rho_m V_m + \rho_c V_c = \rho_m + (\rho_c - \rho_m)\left(\frac{2z+h}{2h}\right)^N, \\ \alpha(z) &= \alpha_m V_m + \alpha_c V_c = \alpha_m + (\alpha_c - \alpha_m)\left(\frac{2z+h}{2h}\right)^N, \end{aligned} \tag{2}$$

The Poisson's ratio ν is assumed to be constant. It is evident from Eq. (2) that the lower surface $\left(z = \frac{h}{2}\right)$ is ceramic-rich, while the top surface $\left(z = -\frac{h}{2}\right)$ is metal-rich, and the rate of the metal constituent in the panel is incremented when (N) rises. When the influence of temperature is studied, the properties of materials of the FGM cylindrical panel can be represented as a non-linear function of the temperature as follows (Hong Cong *et al.* 2017)

$$Pr = P_0(P_{-1}T^{-1} + 1 + P_1T^1 + P_2T^2 + P_3T^3) \tag{3}$$

where $T = T_0 + \Delta T$ and $T_0 = 300$ K (the room temperature), ΔT denoted the temperature rise. While $(P_0, P_{-1}, P_1, P_2, P_3)$ refers to the coefficients characterizing of the constituent materials. In addition, the cylindrical panel resting on the elastic foundations as

$$q_e = K_1 w - K_2 \nabla^2 w, \tag{4}$$

where (q_e) represent the force that is dominated by the foundation, $\nabla^2 = \frac{\partial^2}{\partial^2 x} + \frac{\partial^2}{\partial^2 y}$, (w) describes the deflection of the panel, $K1$, and $K2$ designate to the Winkler and Pasternak Foundation. The different shapes of the stiffeners that will be studied in this research are (Circular, Rectangle, and Triangle) stiffeners as shown in Fig. 1.

3. Theoretical formulation

This section presents the derivation of the equations of motion using the first-order shear deformation theory, which considers that transverse normal deviate from their perpendicular orientation to the mid-surface after deformation. The strain-displacement relationships include the Von Kármán nonlinear terms (Quan *et al*. 2015, Farhan *et al.* 2025)

$$\begin{pmatrix} \varepsilon_x \\ \varepsilon_y \\ \gamma_{xy} \end{pmatrix} = \begin{pmatrix} \varepsilon_x^\circ \\ \varepsilon_y^\circ \\ \gamma_{xy}^\circ \end{pmatrix} + z \begin{pmatrix} \lambda_x \\ \lambda_y \\ \lambda_{xy} \end{pmatrix}, \begin{pmatrix} \gamma_{xz} \\ \gamma_{yz} \end{pmatrix} = \begin{pmatrix} \frac{\partial w}{\partial x} + \phi_x \\ \frac{\partial w}{\partial y} + \phi_y \end{pmatrix}, \tag{5}$$

with

$$\begin{pmatrix} \varepsilon_x^\circ \\ \varepsilon_y^\circ \\ \gamma_{xy}^\circ \end{pmatrix} = \begin{pmatrix} \frac{\partial u}{\partial x} + \frac{1}{2}\left(\frac{\partial w}{\partial x}\right)^2 \\ \frac{\partial v}{\partial y} - \frac{w}{R} + \frac{1}{2}\left(\frac{\partial w}{\partial x}\right)^2 \\ \frac{\partial u}{\partial y} + \frac{\partial v}{\partial x} + \frac{\partial w}{\partial x}\frac{\partial w}{\partial y} \end{pmatrix}, \begin{pmatrix} \lambda_x \\ \lambda_y \\ \lambda_{xy} \end{pmatrix} = \begin{pmatrix} \frac{\partial \phi_x}{\partial x} \\ \frac{\partial \phi_y}{\partial y} \\ \frac{\partial \phi_x}{\partial y} + \frac{\partial \phi_y}{\partial x} \end{pmatrix}, \tag{6}$$

The strains are related to the equation of deformation compatibility

$$\frac{\partial^2 \varepsilon_x{}^\circ}{\partial y^2} + \frac{\partial^2 \varepsilon_y{}^\circ}{\partial x^2} - \frac{\partial^2 \gamma_{xy}^\circ}{\partial x \partial y} = \frac{\partial^2 w^2}{\partial x \partial y} - \frac{\partial^2 w}{\partial x^2}\frac{\partial^2 w}{\partial y^2} + 2\frac{\partial^2 w}{\partial x \partial y}\frac{\partial^2 w^*}{\partial x \partial y} - \frac{\partial^2 w}{\partial x^2}\frac{\partial^2 w^*}{\partial y^2} - \frac{\partial^2 w}{\partial y^2}\frac{\partial^2 w^*}{\partial x^2} - \frac{1}{R}\frac{\partial^2 w}{\partial x^2}, \tag{7}$$

According to Hooke's law, the stress-strain relations are as follows

$$\begin{gathered} \sigma_x^{sh} = \frac{E(z,T)}{1-\nu^2}\left(\varepsilon_x + \nu\varepsilon_y - (1+\upsilon)\alpha(z,T)\Delta T\right), \sigma_y^{sh} = \frac{E(z,T)}{1-\nu^2}\left(\varepsilon_y + \nu\varepsilon_x - (1+\upsilon)\alpha(z,T)\Delta T\right), \\ \sigma_{xy}^{sh} = \frac{E(z,T)}{2(1+\nu)}\gamma_{xy}, \sigma_{xz}^{sh} = K_s\frac{E(z,T)}{2(1+\nu)}\gamma_{xz}, \sigma_{yz}^{sh} = K_s\frac{E(z,T)}{2(1+\nu)}\gamma_{yz}, \end{gathered} \tag{8}$$

where (K_s) is the shear correction factor. Its value (K) is taken as $\left(K = \frac{5}{6}\right)$. The smeared stiffeners method for the contribution of stiffeners is applied in this search. In addition, stress-strain relations for the stiffeners

$$\begin{aligned} \sigma_x^{st} &= E_\circ\left(\frac{\partial u}{\partial x} + \frac{1}{2}\left(\frac{\partial w}{\partial x}\right)^2 + z\frac{\partial \phi_x}{\partial x}\right) - \frac{E_\circ \alpha_\circ(T)\Delta T}{1-2\upsilon}, \\ \sigma_y^{st} &= E_\circ\left(\frac{\partial v}{\partial y} - \frac{w}{R} + \frac{1}{2}\left(\frac{\partial w}{\partial x}\right)^2 + z\frac{\partial \phi_y}{\partial y}\right) - \frac{E_\circ \alpha_\circ(T)\Delta T}{1-2\upsilon}, \end{aligned} \tag{9}$$

When reinforcing the cylindrical panels with the stiffeners toward the (x, y)-axis only, the resultant of the forces and moments are gained as follows

$$N_x = \left(I_{10} + \frac{E_\circ A_x^T}{s_x^T}\right)\varepsilon_x^\circ + I_{20}\varepsilon_y^\circ + (I_{11} + C_x^T)\frac{\partial \phi_x}{\partial x} + I_{21}\frac{\partial \phi_y}{\partial y}, \tag{10a}$$

$$N_y = I_{20}\varepsilon_x^\circ + \left(I_{10} + \frac{E_\circ A_y^T}{s_y^T}\right)\varepsilon_y^\circ + I_{21}\frac{\partial \phi_x}{\partial x} + \left(I_{11} + C_y^T\right)\frac{\partial \phi_y}{\partial y} + \Phi_1, \tag{10b}$$

$$N_{xy} = I_{30}\gamma_{xy}^\circ + 2I_{31}\left(\frac{\partial \phi_x}{\partial y} + \frac{\partial \phi_y}{\partial x}\right), \tag{10c}$$

$$M_x = (I_{11} + C_x^T)\varepsilon_x^\circ + I_{21}\varepsilon_y^\circ + \left(I_{12} + \frac{E_\circ I_x^T}{s_x^T}\right)\frac{\partial \phi_x}{\partial x} + I_{22}\frac{\partial \phi_y}{\partial y} + \Phi_2, \tag{10d}$$

$$M_y = I_{21}\varepsilon_x^\circ + \left(I_{11} + C_y^T\right)\varepsilon_y^\circ + I_{22}\frac{\partial \phi_x}{\partial x} + \left(I_{12} + \frac{E_\circ I_y^T}{s_y^T}\right)\frac{\partial \phi_y}{\partial y} + \Phi_2, \tag{10e}$$

$$M_{xy} = I_{31}\gamma_{xy}^\circ + I_{32}\left(\frac{\partial \phi_x}{\partial y} + \frac{\partial \phi_y}{\partial x}\right), \tag{10f}$$

$$Q_x = K_s I_{30}\gamma_{xz}, (10\,g) \qquad Q_y = K_s I_{30}\gamma_{yz}, \tag{10h}$$

The nonlinear equations of motion for exponentially graded functionally graded material (ES-FGM) cylindrical panels resting on an elastic foundation, formulated using the first-order shear deformation theory in thermal environments, are expressed as follows

$$\delta u: \frac{\partial N_x}{\partial x} + \frac{\partial N_{xy}}{\partial y} = I_0\frac{\partial^2 u}{\partial t^2} + I_1\frac{\partial^2 \phi_x}{\partial t^2}, \tag{11a}$$

$$\delta v: \frac{\partial N_{xy}}{\partial x} + \frac{\partial N_y}{\partial y} = I_0\frac{\partial^2 v}{\partial t^2} + I_1\frac{\partial^2 \phi_y}{\partial t^2}, \tag{11b}$$

$$\delta w: \frac{\partial Q_x}{\partial x} + \frac{\partial Q_y}{\partial y} + N_x\frac{\partial^2 w}{\partial x^2} + 2N_{xy}\frac{\partial^2 w}{\partial x \partial y} + N_y\frac{\partial^2 w}{\partial y^2} + q - K_1 w + K_2\left(\frac{\partial^2 w}{\partial x^2} + \frac{\partial^2 w}{\partial y^2}\right) + \frac{N_y}{R} = I_0\frac{\partial^2 w}{\partial t^2}, \tag{11c}$$

$$\delta \phi_x: \frac{\partial M_x}{\partial x} + \frac{\partial M_{xy}}{\partial y} - Q_x = I_2\frac{\partial^2 \phi_x}{\partial t^2} + I_1\frac{\partial^2 u}{\partial t^2}, \tag{11d}$$

$$\delta \phi_y: \frac{\partial M_{xy}}{\partial x} + \frac{\partial M_y}{\partial y} - Q_y = I_2\frac{\partial^2 \phi_y}{\partial t^2} + I_1\frac{\partial^2 v}{\partial t^2}, \tag{11e}$$

The stress function is presented as

$$N_x = \frac{\partial^2 f}{\partial y^2}, N_y = \frac{\partial^2 f}{\partial x^2}, N_{xy} = -\frac{\partial^2 f}{\partial x \partial y}, \tag{12}$$

$$\frac{\partial^2 u}{\partial t^2} = -\frac{I_1}{I_0}\frac{\partial^2 \phi_x}{\partial t^2}, \frac{\partial^2 v}{\partial t^2} = -\frac{I_1}{I_0}\frac{\partial^2 \phi_y}{\partial t^2}, \tag{13}$$

Replacing Eq. (13) with Eq. (11c)-(11e) yields

$$\delta w: \frac{\partial Q_x}{\partial x} + \frac{\partial Q_y}{\partial y} + N_x\frac{\partial^2 w}{\partial x^2} + 2N_{xy}\frac{\partial^2 w}{\partial x \partial y} + N_y\frac{\partial^2 w}{\partial y^2} + q - K_1 w + K_2\left(\frac{\partial^2 w}{\partial x^2} + \frac{\partial^2 w}{\partial y^2}\right) + \frac{N_y}{R} = I_0\frac{\partial^2 w}{\partial t^2}, \tag{14a}$$

$$\delta \phi_x: \frac{\partial M_x}{\partial x} + \frac{\partial M_{xy}}{\partial y} - Q_x = \left(I_2 - \frac{{I_1}^2}{I_0}\right)\frac{\partial^2 \phi_x}{\partial t^2}, \tag{14b}$$

$$\delta \phi_y: \frac{\partial M_{xy}}{\partial x} + \frac{\partial M_y}{\partial y} - Q_y = \left(I_2 - \frac{{I_1}^2}{I_0}\right)\frac{\partial^2 \phi_y}{\partial t^2}, \tag{14c}$$

Through Eqs. (10a)-(10c) produce

$$\gamma_{xy}^{\circ} = A_{66}N_{xy} - B_{66}\left(\frac{\partial \phi_x}{\partial y} + \frac{\partial \phi_y}{\partial x}\right), \tag{15}$$

Inserting Eq. (15) into Eqs. (10d)-(10h), and then into Eq. (14) leads to

$$R_{11}(w) + R_{12}(\phi_x) + R_{13}(\phi_y) + S_1(w, f) + q = I_0\frac{\partial^2 w}{\partial t^2}, \tag{16a}$$

$$R_{21}(w) + R_{22}(\phi_x) + R_{23}(\phi_y) + S_2(f) = \left(I_2 - \frac{{I_1}^2}{I_0}\right)\frac{\partial^2 \phi_x}{\partial t^2}, \tag{16b}$$

$$R_{31}(w) + R_{32}(\phi_x) + R_{33}(\phi_y) + S_3(f) = \left(I_2 - \frac{{I_1}^2}{I_0}\right)\frac{\partial^2 \phi_y}{\partial t^2}, \tag{16c}$$

From Eq. (15) in conjunction with the equation of the stress functions, substituting Eq. (15) into Eq. (7) provides the equation of compatibility of imperfect FGM cylindrical panels as

$$\begin{aligned} &A_{11}\frac{\partial^4 f}{\partial x^4} + A_{22}\frac{\partial^4 f}{\partial y^4} + (A_{66} - 2A_{12})\frac{\partial^4 f}{\partial x^2 \partial y^2} - B_{21}\frac{\partial^3 \phi_x}{\partial x^3} - B_{12}\frac{\partial^3 \phi_y}{\partial y^3} + (B_{66} - B_{11})\frac{\partial^3 \phi_x}{\partial x \partial y^2} + \\ &(B_{66} - B_{22})\frac{\partial^3 \phi_y}{\partial x^2 \partial y} - \left(\frac{\partial^2 w^2}{\partial x \partial y} - \frac{\partial^2 w}{\partial x^2}\frac{\partial^2 w}{\partial y^2} + 2\frac{\partial^2 w}{\partial x \partial y}\frac{\partial^2 w^*}{\partial x \partial y} - \frac{\partial^2 w}{\partial x^2}\frac{\partial^2 w^*}{\partial y^2} - \frac{\partial^2 w}{\partial y^2}\frac{\partial^2 w^*}{\partial x^2} - \frac{1}{R}\frac{\partial^2 w}{\partial x^2}\right) = 0, \end{aligned} \tag{17}$$

Eqs. (16) and (17) define the nonlinear relationships through the variables are used to analyze the nonlinear vibration behavior of functionally graded thick cylindrical shells resting on elastic foundations in thermal environments, based on the first-order shear deformation theory (FSDT).

4. Formulation to analyze the natural frequency

The problem was formulated for simply supported boundary conditions. For a UDL force and implementing the boundary condition the following forms were obtained

$$\begin{aligned} &w = N_{xy} = \phi_y = 0, N_x = N_{x0}, at\ x = 0, a, \\ &w = N_{xy} = \phi_x = 0, N_y = N_{y0}, at\ y = 0, b, \end{aligned} \tag{18}$$

To satisfy the conditions given in Eq. (18), the mode shape is expressed as follows

$$\begin{aligned} &w(x, y, t) = W(t)\sin\lambda_m x \sin\delta_n y, \\ &\phi_x(x, y, t) = \Phi_x(t)\cos\lambda_m x \sin\delta_n y, \\ &\phi_y(x, y, t) = \Phi_y(t)\sin\lambda_m x \cos\delta_n y, \end{aligned} \tag{19}$$

And for initial imperfection

$$w^*(x, y) = W_{\circ}\sin\lambda_m x \sin\delta_n y, \tag{20}$$

To find the coefficients of the stress function substituting Eqs. (19) & (20) into Eq. (17) we obtain

$$\begin{aligned} \tilde{f}(x, y, t) = \tilde{A}_1(t)\cos 2\lambda_m x + \tilde{A}_2(t)\cos 2\delta_n y + \tilde{A}_3(t)\sin\lambda_m x \sin\delta_n y + \frac{1}{2}N_{x0}y^2 + \\ \frac{1}{2}N_{y0}x^2, \end{aligned} \tag{21}$$

where

$$\tilde{A}_1(t)=\frac{\delta_n^2}{32A_{11}\lambda_m^2}W(W+2W_\circ),\tilde{A}_2(t)=\frac{\lambda_m^2}{32A_{22}\delta_n^2}W(W+2W_\circ),$$
$$\tilde{A}_3(t)=\frac{1}{[A_{11}\lambda_m^4+A_{22}\delta_n^4+(A_{66}-2A_{12})\lambda_m^2\delta_n^2]}\frac{W}{R}$$
$$+\frac{[B_{21}\lambda_m^3+(B_{11}-B_{66})\lambda_m\delta_n^2]\Phi_x(t)+[\delta_n^3B_{12}+(B_{22}-B_{66})\lambda_m^2\delta_n]\Phi_y(t)}{[A_{11}\lambda_m^4+A_{22}\delta_n^4+(A_{66}-2A_{12})\lambda_m^2\delta_n^2]}, \tag{22}$$

Consider the (ES-FGM) thick cylindrical panel with four edges which are simply supported and immovable subjected to thermal loads. The conditions displaying of the immovable on edges is $u=0$ on $x=0,a$ and $v=0$ on $y=0,b$

$$\int_0^a\int_0^b\frac{\partial u}{\partial x}dxdy=0,\int_0^a\int_0^b\frac{\partial v}{\partial y}dxdy=0, \tag{23}$$

From Eq. (6) and Eq. (15) in conjunction with the equation of the stress functions, can obtain the resulting expressions

$$\frac{\partial u}{\partial x}=A_{22}\frac{\partial^2 f}{\partial y^2}-A_{12}\frac{\partial^2 f}{\partial x^2}-B_{11}\frac{\partial\phi_x}{\partial x}-B_{12}\frac{\partial\phi_y}{\partial y}-\frac{1}{2}\left(\frac{\partial w}{\partial x}\right)^2-\frac{\partial w}{\partial x}\frac{\partial w_\circ}{\partial x}+C_{11}^*\Phi_1,$$
$$\frac{\partial v}{\partial y}=A_{11}\frac{\partial^2 f}{\partial x^2}-A_{12}\frac{\partial^2 f}{\partial y^2}-B_{21}\frac{\partial\phi_x}{\partial x}-B_{22}\frac{\partial\phi_y}{\partial y}+\frac{w}{R}-\frac{1}{2}\left(\frac{\partial w}{\partial y}\right)^2-\frac{\partial w}{\partial y}\frac{\partial w_\circ}{\partial y}+C_{22}^*\Phi_1, \tag{24}$$

Substituting Eqs. (19)-(21) into Eq. (24), after that the results replacing into Eq. (23), provides

$$N_{x0}=\frac{4\delta_n}{\lambda_m ab}\tilde{A}_3-\frac{4}{\delta_n ab}\frac{(B_{21}A_{12}+A_{11}B_{11})}{H_{11}}\Phi_x-\frac{4}{\lambda_m ab}\frac{(B_{22}A_{12}+A_{11}B_{12})}{H_{11}}\Phi_y-\frac{4}{\delta_n\lambda_m R}\frac{A_{12}}{H_{11}}W+$$
$$\frac{\delta_n\lambda_m}{8ab}\frac{(\delta_n^2A_{12}+\lambda_m^2A_{11})}{H_{11}}W^2+\frac{\delta_n\lambda_m}{4ab}\frac{(\delta_n^2A_{12}+\lambda_m^2A_{11})}{H_{11}}WW_\circ-\frac{(C_{11}^*A_{11}+C_{22}^*A_{12})}{H_{11}}\Phi_1, \tag{25a}$$

$$N_{y0}=\frac{4\lambda_m}{\delta_n ab}\tilde{A}_3-\frac{4}{\delta_n ab}\frac{(B_{11}A_{12}+A_{11}A_{22}B_{21})}{H_{11}}\Phi_x-\frac{4}{\lambda_m ab}\frac{(B_{12}A_{12}+A_{22}B_{22})}{H_{11}}\Phi_y-\frac{4}{\delta_n\lambda_m R}\frac{A_{22}}{H_{11}}W+$$
$$\frac{\delta_n\lambda_m}{8ab}\frac{(\lambda_m^2A_{12}+\delta_n^2A_{22})}{H_{11}}W^2+\frac{\delta_n\lambda_m}{4ab}\frac{(\delta_n^2A_{12}+\lambda_m^2A_{22})}{H_{11}}WW_\circ-\frac{(C_{11}^*A_{12}+C_{22}^*A_{22})}{H_{11}}\Phi_1, \tag{25b}$$

Then, substituting Eqs. (19)-(21), and Eq. (25) into Eq. (16), after that applying Galerkin's approach leads to

$$r_{11}W+r_{12}\Phi_x+r_{13}\Phi_y+r_{14}(W+W_\circ)\Phi_x+r_{15}(W+W_\circ)\Phi_y+r_{16}(W+W_\circ)+r_{17}W^2+$$
$$r_{18}WW_\circ+r_{19}W^3+r_{110}W^2W_\circ+r_{111}WW_\circ^2+H_{32}q=I_0\frac{d^2W}{dt^2}, \tag{26a}$$

$$r_{21}W+r_{22}\Phi_x+r_{23}\Phi_y+n_7(W+W_\circ)+n_8W(W+2W_\circ)=\tilde{\rho}_1\ddot{\Phi}_x, \tag{26b}$$

$$r_{31}W+r_{32}\Phi_x+r_{33}\Phi_y+n_9(W+W_\circ)+n_{10}W(W+2W_\circ)=\tilde{\rho}_1\ddot{\Phi}_y, \tag{26c}$$

The natural frequencies can be derived by solving the below equation for perfect panel state ($q=0$)

$$\begin{vmatrix} r_{11}+r_{16}+I_0\omega^2 & r_{12} & r_{13} \\ r_{21}+n_7 & r_{22}+\tilde{\rho}\omega^2 & r_{23} \\ r_{31}+n_9 & r_{32} & r_{33}+\tilde{\rho}_1\omega^2 \end{vmatrix}=0, \tag{27}$$

Solving Eq. (27) yields three angular frequencies for the functionally graded material (FGM) cylindrical panel, corresponding to the circumferential, radial, and axial directions. The smallest of

these values is considered for analysis.

5. Formulation for nonlinear dynamic responses

Consider an FGM cylindrical shell subjected to a uniformly distributed transverse load, expressed as ($q = Q\ \sin\Omega t$). Under this loading condition, the nonlinear Eq. (26) are modified as follows

$$I_0\frac{d^2W}{dt^2} - r_{11}W - r_{12}\Phi_x - r_{13}\Phi_y - r_{14}(W+W_\circ)\Phi_x - r_{15}(W+W_\circ)\Phi_y r_{16}(W+W_\circ) - r_{17}W^2 - r_{18}WW_\circ - r_{19}W^3 - r_{110}W^2W_\circ - r_{111}WW_\circ^2 = H_{32}Q\,sin\,\Omega\,t, \tag{28a}$$

$$r_{21}W + r_{22}\Phi_x + r_{23}\Phi_y + n_7(W+W_\circ) + n_8W(W+2W_\circ) = \tilde{\rho}_1\ddot{\Phi}_x, \tag{28b}$$

$$r_{31}W + r_{32}\Phi_x + r_{33}\Phi_y + n_9(W+W_\circ) + n_{10}W(W+2W_\circ) = \tilde{\rho}_1\ddot{\Phi}_y, \tag{28c}$$

By utilizing Eq. (28), which accounts for three key characteristics, the frequency-amplitude relationship for nonlinear free vibration can be determined. This equation also provides the fundamental frequencies of exponentially graded functionally graded material (ES-FGM) cylindrical panels and describes their nonlinear dynamic responses. The nonlinear dynamic behavior of ES-FGM panels can be obtained by solving Eq. (28) under specified initial conditions $\left(W(0)=0, \dot{W}(0)=0\right)$ by applying the Runge-Kutta method. For further study, we next examine the virtual case of rotations $\left(\Phi_x, \Phi_y\right)$ exist, but the inertial forces produced by the rotation angles $\left(\Phi_x, \Phi_y\right)$ are small so they can be neglected. The Eq. (3.28) can be rewritten as

$$I_0\frac{d^2W}{dt^2} - r_{11}W - r_{12}\Phi_x - r_{13}\Phi_y - r_{14}(W+W_\circ)\Phi_x - r_{15}(W+W_\circ)\Phi_y r_{16}(W+W_\circ) - r_{17}W^2 - r_{18}WW_\circ - r_{19}W^3 - r_{110}W^2W_\circ - r_{111}WW_\circ^2 = H_{32}Q\,sin\,\Omega\,t, \tag{29a}$$

$$r_{21}W + r_{22}\Phi_x + r_{23}\Phi_y + n_7(W+W_\circ) + n_8W(W+2W_\circ) = 0, \tag{29b}$$

$$r_{31}W + r_{32}\Phi_x + r_{33}\Phi_y + n_9(W+W_\circ) + n_{10}W(W+2W_\circ) = 0, \tag{29c}$$

From Eq. (29), solving the second and third equations with respect to Φ_x and Φ_y then replaced the results into the first equation yields

$$I_0\frac{d^2W}{dt^2} - a_1W - a_2(W+W_\circ) - a_3W(W+W_\circ) - a_4W(W+2W_\circ) - a_5W(W+W_\circ)(W+2W_\circ) - a_6(W+W_\circ)^2 - r_{17}W^2 - r_{18}WW - r_{19}W^3 - r_{110}W^2W_\circ - r_{111}WW_\circ^2 = H_{32}Q\,sin\,\Omega\,t, \tag{30}$$

For a perfect panel, Eq. (3.30) becomes as

$$I_0\frac{d^2W}{dt^2} - (a_1+a_2)W - (a_3+a_4+a_6+r_{17})W^2 - (a_5+r_{19})W^3 = H_{32}Q\,sin\,\Omega\,t, \tag{31}$$

For an ideal shell, the fundamental frequencies can be obtained as

$$\omega_{mn} = \sqrt{\frac{-(a_1+a_2)}{I_0}}, \tag{32}$$

Eq. (31) can be rewritten as follows

Table 1 Validation results

a/R	*N*	Ref. (Chorfi and Houmat 2010)	Ref. (Bich *et al.* 2012)	Present (FSDT)	Difference (%)
FGM plate 0	0	0.0577	0.0597	0.0589	1.34
	0.5	0.049	0.0506	0.0498	1.58
	1	0.0422	0.0456	0.0499	9.42
	4	0.04830	0.0396	0.0389	1.76
FGM cylindrical panel 0.5	0	0.0629	0.0648	0.0639	1.38
	0.5	0.054	0.0553	0.0545	1.44
	1	0.049	0.0501	0.0493	1.59
	4	0.0419	0.0430	0.0423	1.62

$$\frac{d^2W}{dt^2} + \omega_{mn}^2\left(W - \tilde{M}W^2 + \tilde{N}W^3\right) - \tilde{F}\,sin\,\Omega\,t = 0, \tag{33}$$

where

$$\tilde{M} = -\frac{(a_3+a_4+a_6+r_{17})}{(a_1+a_2)}, \tilde{N} = \frac{(a_5+r_{19})}{(a_1+a_2)}, \tilde{F} = \frac{H_{32}Q}{I_0}, \tag{34}$$

For seeking the frequency-amplitude relationship properties of the non-linear vibration, replacing $\left(W = \tilde{A}\,\sin\Omega t\right)$ into Eq. (33), after that employing Galerkin's approach which means multiplying this equation by $(\sin\Omega t)$ and then integrate the results from $(0\ \text{to}\ \pi/2\Omega)$, the frequency-amplitude relationship of nonlinear forced vibration can be written as follows

$$\Omega^2 - \omega_{mn}^2\left(1 - \frac{8}{3\pi}\tilde{M}\tilde{A} + \frac{3\tilde{N}}{4}\tilde{A}^2\right) = -\frac{\tilde{F}}{\tilde{A}}, \tag{35}$$

By indicating $\left(\beta = \frac{\Omega}{\omega_{\mathrm{mn}}}\right)$ represented the frequency ratio, Eq. (35) becomes as

$$\beta^2 - \left(1 - \frac{8}{3\pi}\tilde{M}\tilde{A} + \frac{3\tilde{N}}{4}\tilde{A}^2\right) = -\frac{\tilde{F}}{\tilde{A}\omega_{mn}^2}, \tag{36}$$

In the case of nonlinear free vibrations (no excitation force) on the panel, $\left(\tilde{F} = 0\right)$. The frequency-amplitude relation of nonlinear free vibration is found as follows

$$\omega_{NL}^2 = \omega_{mn}^2\left(1 - \frac{8}{3\pi}\tilde{M}\tilde{A} + \frac{3\tilde{N}}{4}\tilde{A}^2\right), \tag{37}$$

6. Numerical results and discussions

6.1 Validation

The functionally graded material of the current study is assumed as (Cong *et al.* 2017). Consider an (ES-FGM) cylindrical panel acted by the uniformly transverse distributed load $(q = Q\,\sin\Omega t)$ where (Q) represented the amplitude of uniformly excited load, (Ω) refer to the frequency of the load. The Runge-Kutta approach is utilized to solve Eq. (28). To validate the accuracy and efficiency of the first-order shear deformation theory method without thermal

Table 2 Validation results of FGM plate resting on an elastic foundation in a thermal environment

(K_1, K_2)(GPa/m,GPa/m)	ΔT(°C)	Ref. (Mouthanna *et al.* 2018)	Present (FSDT)	Difference %
0.25, 0.02	0	2779.46	2607.6	6.1
	50	2533.92	2453.2	3.18
	105	2232.86	2265.2	1.44

Table 3 Influence of the Winkler and Pasternak foundations on the natural frequency for the (P-FGM) cylindrical panel without thermal environment a=b=1.5 m, N=5, R=3 m, h=0.008 m

(K_1, K_2) GPa/m	Natural frequency (Hz)		
	Circular stiffeners	Rectangle stiffeners	Triangle stiffeners
(0,0)	1091.4	1094.4	1092.4
(0.3,0)	3766.9	3767.7	3767.4
(0.3,0.02)	4668.1	4668.8	4668.4
(0.3,0.04)	5421.6	5422.2	5421.8

environment effects following analysis has been performed and shown in Table 2. The Table 2 explains the comparison between the present approach adopted (FSDT) and the results of (Matsunaga 2008) according to the 2D-higher-order theory and (Bich *et al.* 2012) that used the first-order shear deformation theory approach. The results show that there is not a big difference in this comparison study. Table 3 compares the values of the natural frequency under the thermal environment of the FGM plate (a/b=1, (m, n)=(1,1), a/h=20 and N=1) together with (Duc *et al.* 2016) based on third-order shear deformation theory. The results presented are very compatible with those of published literature.

6.2 Effect of power law index N

From Fig. 2 it is concluded that the three forms of stiffeners have similar behavior in the time-deflection curves under the influence of power index increase and the difference between them is slight.

The material properties of the present study are graded towards the thickness according to power law distribution (P-FGM) depending on the volume fraction index (N) as mentioned previously. The effect of power index (N) on the amplitude of nonlinear vibration for a structure in the shape of a cylindrical panel made of FGM and reinforced by stiffeners is provided in Figure 2. The results explain that the response of the vibration decreases when the power index is 1, while there are increase in the vibration amplitude if the power index is higher than 3. This is because the increase in the volume fraction index leads to an increase in the properties of the metal, that the modulus of elasticity of the metal is less than the ceramic.

6.3 Effect of elastic foundations

A key objective of this research is to achieve a high natural frequency while minimizing the vibration amplitude in the nonlinear dynamic response of P-FGM cylindrical panels. However, not all high vibrations are undesirable, as certain applications require elevated vibration levels. In the

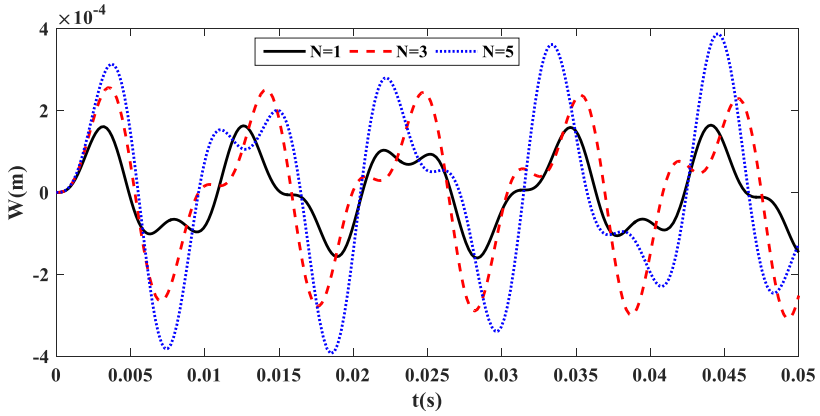

(a) Circular stiffeners

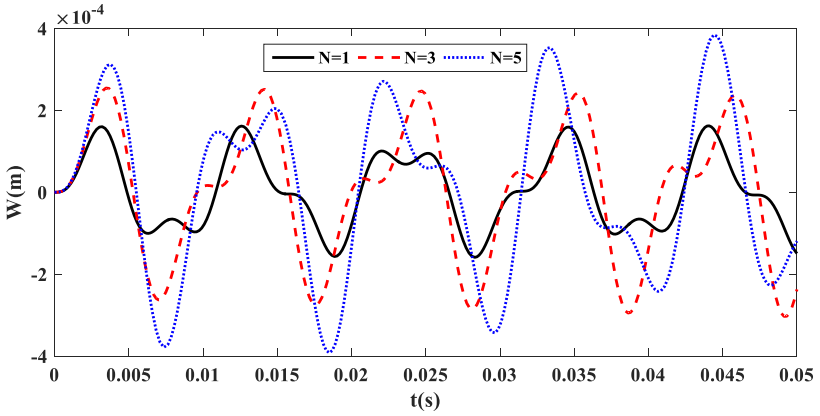

(b) Rectangle stiffeners

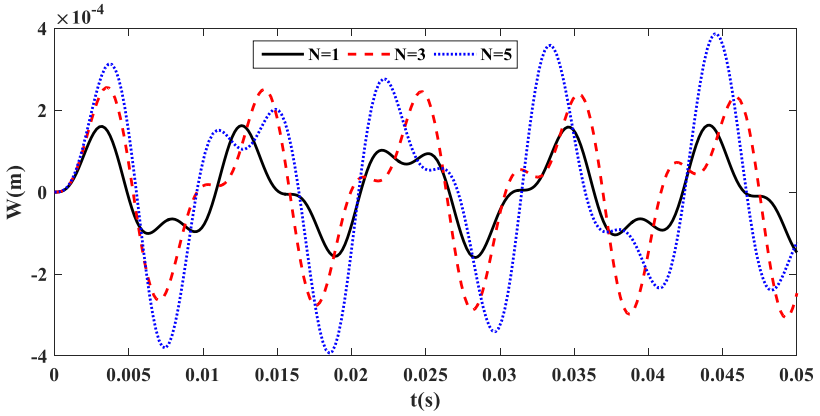

(c) Triangle stiffeners

Fig. 2 Effect of power index (N) on nonlinear vibration response for FGM cylindrical panel without thermal environment a=b=1.5 m, R=3 m, h=0.008 m, $K1$=$K2$=0, q_0=3000 sin 600t, $W0$=0

context of this study, engineering structures must maintain low vibration amplitudes to prevent potential failure and ensure structural integrity.

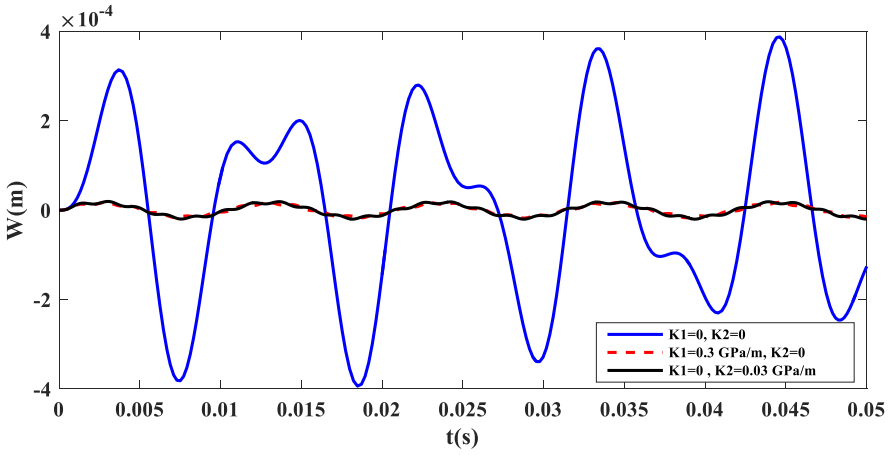

(a) Circular stiffeners

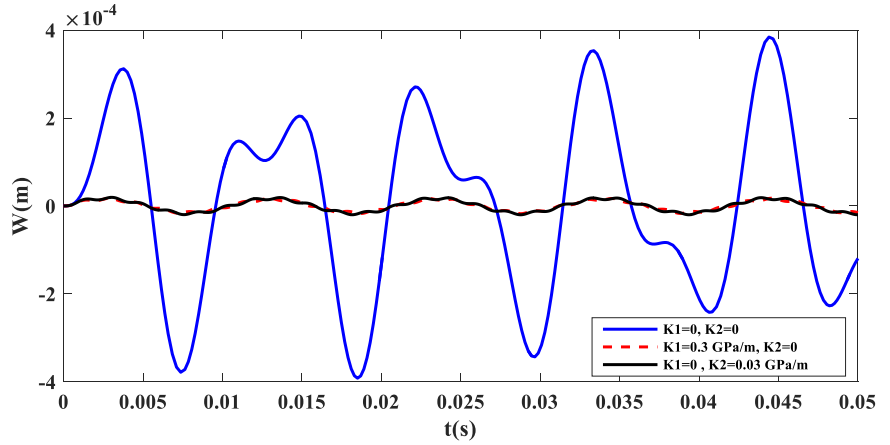

(b) Rectangle stiffener

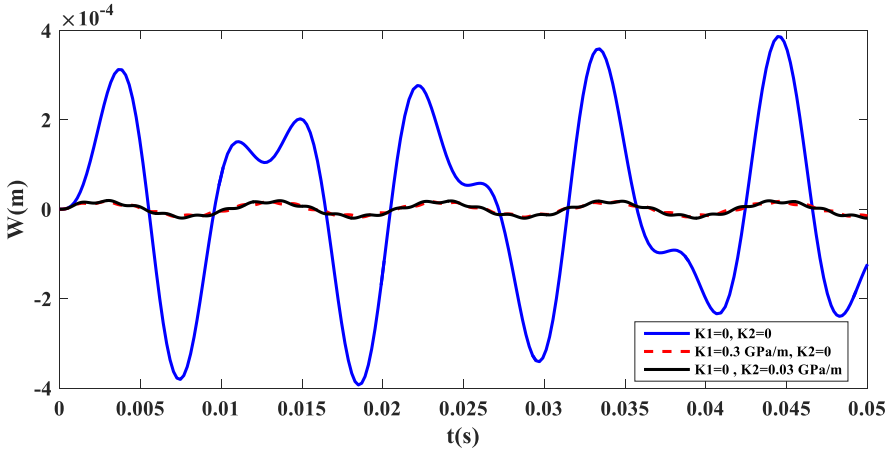

(c) Triangle stiffeners

Fig. 3 Comparison between the effect of Winkler and Pasternak foundation parameters on the amplitude of nonlinear vibration for (ES-FGM) cylindrical panel without thermal environment a=b=1.5 m, N=1, R=3 m, h=0.008, q_0=3000sin600t

Table 4 Influence of temperature field on the natural frequency for the (P-FGM) cylindrical panel a=b=1.5 m, N=1, R=3 m, h=0.008, $K1$=$K2$=0

$\Delta T\ (K)$	Natural frequency (Hz)		
	Circular stiffeners	Rectangle stiffeners	Triangle stiffeners
0	1188.5	1193.5	1190.4
50	1033.9	1039.7	1036.4
150	845.92	852.98	848.52
200	549.87	604.72	598.55

The impact of the linear Winkler and Pasternak foundations on the natural frequency for the functionally graded cylindrical panel without a thermal environment reinforced by different stiffeners is described in Table 3. It is concluded that the elastic foundation has a major effect on the natural frequency. Increasing the value of the elastic foundation leads to an increase in the natural frequency. It can also be observed that the difference between the three forms of the stiffeners is very small and this will be seen when the influence of the elastic foundation is found on the time-deflection curve.

In addition, from Fig. 3, when $\left(K_1 = 0.3\ \frac{\mathrm{GPa}}{\mathrm{m}}\ \text{and}\ K_2 = 0.03\ \frac{\mathrm{GPa}}{\mathrm{m}}\right)$, the time-deviation curve can be observed at the same level. It is concluded that the Pasternak parameter $K2$ (shear layer stiffness) has a stronger effect than the Winkler parameter $K1$ on the amplitude of nonlinear vibration for the P-FGM cylindrical panel. The elastic foundation has a positive impact on decreasing the amplitude vibration.

6.4 Results of thermal environment

Because of the nature of this type of material which is used in thermal environment applications, the effect of temperature on the natural frequency and the behavior of the amplitude of the nonlinear dynamic response of this structure should be studied. Table 1 presents the properties of the materials used in this part

The impact of the temperature increment (ΔT) on the natural frequencies for (ES-FGM) thick cylindrical panels under thermal environments without elastic foundation is illustrated in Table 4. Through this table, it is observed that the temperature has a very significant influence on natural frequencies. The value of natural frequency decreases when the value of temperature increases in the three cases of reinforcement. It is concluded that the structure will become less rigid and its performance will decrease, adding to the high probability of failure.

Fig. 4. describes the behavior of vibration amplitude under the influence of increasing temperature. The results display that the deflection increases with the increase of temperature in all states of reinforcement (circular, rectangle, and triangle). Therefore, the temperature has a positive effect on the nonlinear dynamic response. Through Fig. 4, it can be seen that when the temperature rises to (105 K), the amplitude of (ES-FGM) approximately increases $(4.904 \times 10^{-4}\ \mathrm{m})$.

Table 5 represents the influence of the elastic foundation and temperature on the natural frequency for (ES-FGM) thick cylindrical panel under a thermal environment for three forms of the stiffener. Three values are selected for the effect of Winkler parameter and the same values for Pasternak effect to determine the difference between these effects with increased temperature. The first point that can be seen from Table 5 is that high temperatures lead to a reduction in natural

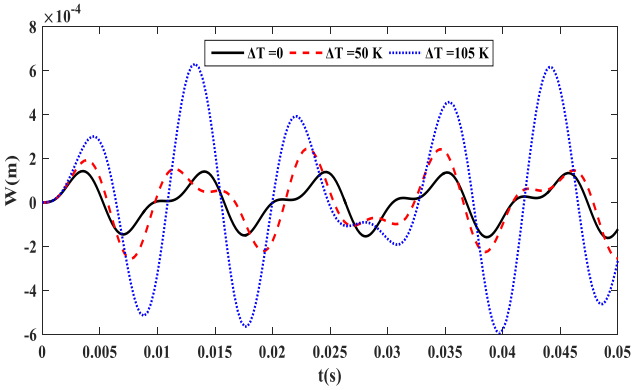

(a) Circular stiffeners

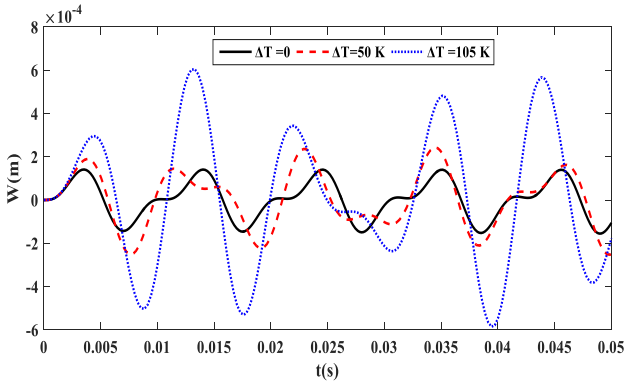

(b) Rectangle stiffeners

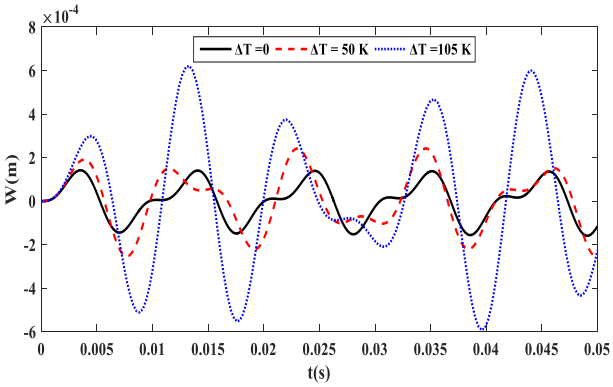

(c) Triangle stiffeners

Fig. 4 Effect of increasing temperature on the amplitude of nonlinear vibration response for the (P-FGM) cylindrical panel a=b=1.5 m, N=1, R=3 m, h=0.008, $K1$=$K2$=0, q=3000sin600t

frequencies. The second point is that the increase in elastic foundation coefficients leads to an increment in natural frequencies under the influence of temperature. In other words, the load-carrying capacity will be improved when the parameters of the elastic foundation increase. The last point is the difference between the Winkler and Pasternak effects on natural frequencies. The

Table 5 Effect of the elastic foundation parameter and temperature on the natural frequency for (ES-FGM) cylindrical panel a=b=1.5 m, N=1, R=3 m, h=0.008

(K_1, K_2) GPa/m	ΔT (K)	Circular stiffeners	Rectangle stiffeners	Triangle stiffeners
(0,0)	0	1188.5	1193.5	1190.4
	100	845.29	852.98	848.52
(0.01,0)	0	1284.5	1289.1	1286.2
	100	976.14	982.27	978.4
(0.03,0)	0	1457.5	1461.6	1459
	100	1194.8	1199.8	1196.6
(0,0.01)	0	1869.3	1872.5	1870.5
	100	1672.5	1676.1	1673.8
(0,0.03)	0	2767.2	2769.4	2768.0
	100	2638.3	2640.6	2639.1

results show that the shear layer (Pasternak foundation) has a bigger influence than the Winkler foundation because Winkler's proposal eliminates the effect of the sheer that occurs in the foundation.

6.5 Effect of angular velocity

The effect of angular velocity on the t(s)-W(m) time-deflection curve for the (ES-FGM) cylindrical panel is illustrated in Fig. 5. The deflection curve has a special pattern when the natural frequency is approaching the excited frequency. The natural frequency is $\left(\omega = 1901.4\frac{\text{rad}}{\text{s}}\omega = 1094.4\frac{\text{rad}}{\text{s}}\omega = 1092.2\frac{\text{rad}}{\text{s}}\right)$ for the circular, rectangle, and triangle stiffeners respectfully. Through the figures obtained, it can be noted that the beating vibration phenomenon occurs because the excitation frequency is near to the natural frequency of the FGM cylindrical panel for three forms of reinforcement. Increasing the angular velocity leads to a reduction in the number of beats in the scheme of time-deflection for three cases of stiffeners.

7. Conclusions

The governing equations of the eccentrically stiffened for the cylindrical panel made of advanced material which is functionally graded material and reinforced with different modes of the stiffeners for both longitudinal and transverse directions were derived based on the first-order shear deformation theories. Also, applied the smeared stiffeners method with the von Karman terms. The effect of the thermal environment and elastic foundation on the amplitude of nonlinear dynamic responses and natural frequencies was analyzed. Galerkin's procedure is used for the analysis of the dynamic properties of ES-FGM cylindrical shells. Nonlinear dynamic responses of (ES-FGM) cylindrical shells are investigated according to the fourth-order Runge-Kutta. The elastic foundation has a useful impact on the natural frequency and vibration amplitude. Raising the value of the elastic foundation leads to an increase in the natural frequency and a decrease in the amplitude of the nonlinear dynamic response. The Pasternak Foundation has a larger impact than the Winkler Foundation. The natural frequency decreases when the value of temperature

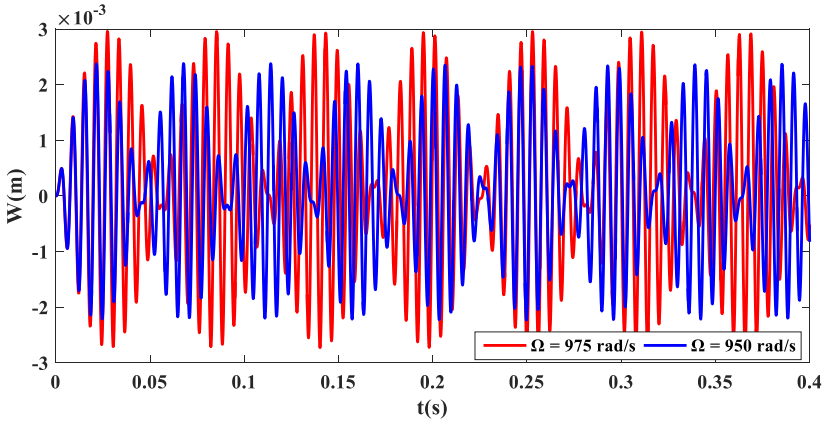

(a) Circular stiffeners

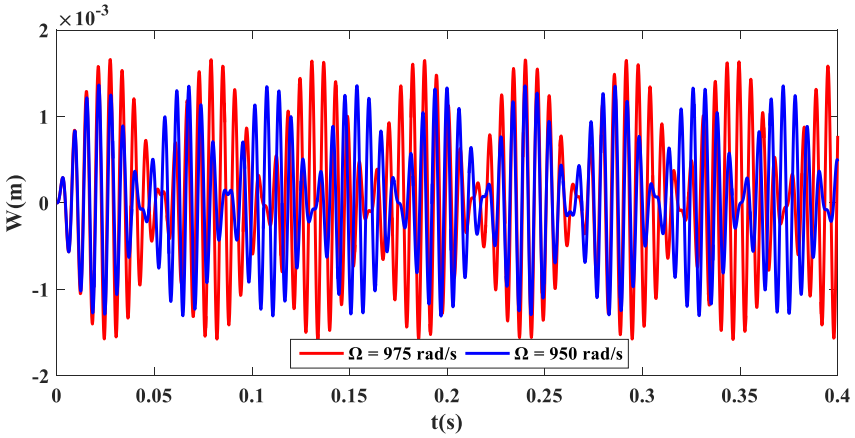

(b) Rectangle stiffeners

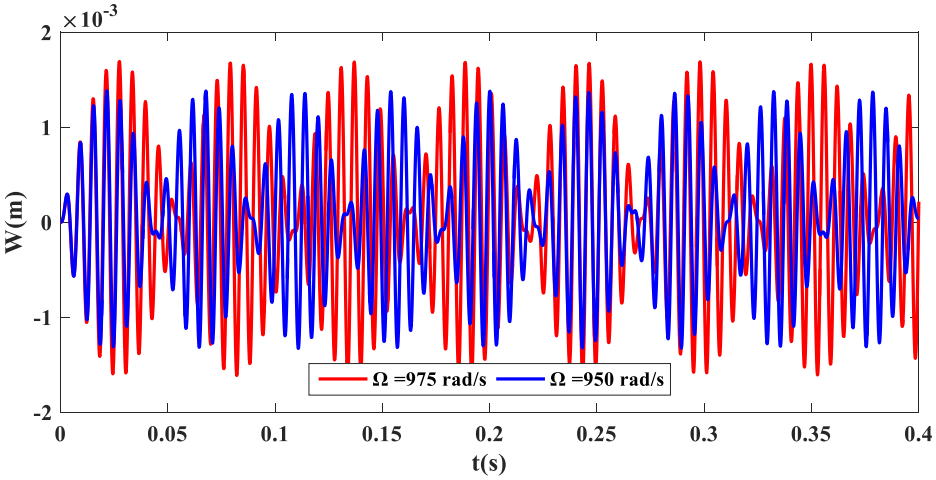

(c) Triangle stiffeners

Fig. 5 Nonlinear response of (ES-FGM) cylindrical panel without thermal environment h=0.008 m, R=3 m, N=5, $K1$=$K2$=0, $q0$=5000sinΩt

increases, and the amplitude of the non-linear vibration response increases when the value of the temperature increases. Using an analytical approach, the Runge-Kutta method, the Galerkin method, and the stress function, the nonlinear dynamic features of the ES-FGM cylindrical panels are calculated by explicit relations among geometrical parameters, stiffeners, elastic foundations, and temperature, so we can vigorously control vibration and the dynamic response of the ES-FGM cylindrical panels by suitable pre-selection of these parameters.

References

Ali, A.Y. and Hasan, H.M. (2019), "Nonlinear dynamic stability of an imperfect shear deformable orthotropic functionally graded material toroidal shell segments under the longitudinal constant velocity", *Proc. Inst. Mech. Eng., Part C: J. Mech. Eng. Sci.*, **233**(19-20), 6827-6850. https://doi.org/10.1177/0954406219867991.

Ali, A.Y. and Hasan, H.M. (2022), "Non-linear large amplitude vibration of orthotropic FGM convex and concave toroidal shell segments including the damping effect using the shear deformation theory", *Thin Wall. Struct.*, **173**, 109035. https://doi.org/10.1016/j.tws.2022.109035.

Arefi, M., Karroubi, R. and Irani-Rahaghi, M. (2016), "Free vibration analysis of functionally graded laminated sandwich cylindrical shells integrated with piezoelectric layer", *Appl. Math. Mech.*, **37**(7), 821-834. https://doi.org/10.1007/s10483-016-2098-9.

Bayat, M., Sahari, B.B., Saleem, M., Ali, A. and Wong, S.V. (2009), "Bending analysis of a functionally graded rotating disk based on the first order shear deformation theory", *Appl. Math. Model.*, **33**(11), 4215-4230. https://doi.org/10.1016/j.apm.2009.03.001.

Bich, D.H. and Long, V.D. (2007), "Non-linear dynamical analysis of laminated reinforced composite doubly curved shallow shells", *Viet. J. Mech.*, **29**(3), 257-269. https://doi.org/10.15625/0866-7136/29/3/5538.

Bich, D.H., Dung, D.V. and Nam, V.H. (2012), "Nonlinear dynamical analysis of eccentrically stiffened functionally graded cylindrical panels", *Compos. Struct.*, **94**(8), 2465-2473. https://doi.org/10.1016/j.compstruct.2012.03.012.

Chorfi, S.M. and Houmat, A. (2010), "Non-linear free vibration of a functionally graded doubly-curved shallow shell of elliptical plan-form", *Compos. Struct.*, **92**(10), 2573-2581. https://doi.org/10.1016/j.compstruct.2010.02.001.

Daneshmand, S., Vini, M.H., Sajadi, S.M., Mouthanna, A., Jasim, D.J., Hammoodi, K.A., Hekmatifar, M. and Nasajpour-Esfahani, N. (2023), "Numerical and experimental investigations of mechanical, tribological, and electrical properties of laminated Bi-metal Al/SiC/Ni composites", *Mater. Today Commun.*, **37**, 107355. https://doi.org/10.1016/j.mtcomm.2023.107355.

Deniz, A., Zerin, Z. and Karaca, Z. (2016), "Winkler-Pasternak foundation effect on the frequency parameter of FGM truncated conical shells in the framework of shear deformation theory", *Compos. Part B: Eng.*, **104**, 57-70. https://doi.org/10.1016/j.compositesb.2016.08.006.

Duc, N.D. and Thang, P.T. (2015), "Nonlinear dynamic response and vibration of shear deformable imperfect eccentrically stiffened S-FGM circular cylindrical shells surrounded on elastic foundations", *Aerosp. Sci. Technol.*, **40**, 115-127. https://doi.org/10.1016/j.ast.2014.11.005.

Duc, N.D. and Tung, H.V. (2010), "Nonlinear analysis of stability for functionally graded cylindrical panels under axial compression", *Fifth Conference of the Asian Consortium for Computational Materials Science ACCMS-5*, Hanoi, Vietnam, September.

Duc, N.D., Bich, D.H. and Cong, P.H. (2016), "Nonlinear thermal dynamic response of shear deformable FGM plates on elastic foundations", *J. Therm. Stress.*, **39**(3), 278-297.

Ellali, M., Amara, K. and Bouazza, M. (2024), "Thermal buckling of porous FGM plate integrated surface-bonded piezoelectric", *Couple. Syst. Mech.*, **13**(2), 171-186. https://doi.org/10.12989/csm.2024.13.2.171.

Farhan, Z.A., Jweeg, M.J., Njim, E.K., Mouthanna, A., Mujtaba, A.F., Royal, M., Khobragade, P. and

Kumar, R.P. (2025), "Nonlinear frequency and dynamic response of PLA polymeric imperfect FG sandwich plates under hygrothermal conditions", *Couple. Syst. Mech.*, **14**(1), 1-19. https://doi.org/10.12989/csm.2025.14.1.001.

Gao, K., Gao, W., Wu, D. and Song, C. (2018), "Nonlinear dynamic stability of the orthotropic functionally graded cylindrical shell surrounded by Winkler-Pasternak elastic foundation subjected to a linearly increasing load", *J. Sound Vib.*, **415**, 147-168. https://doi.org/10.1016/j.jsv.2017.11.038.

Hong Cong, P., Anh, V.M. and Dinh Duc, N. (2017), "Nonlinear dynamic response of eccentrically stiffened FGM plate using Reddy's TSDT in thermal environment", *J. Therm. Stress.*, **40**(6), 704-732. https://doi.org/10.1080/01495739.2016.1261614.

Huy Bich, D., Dinh Duc, N. and Quoc Quan, T. (2014), "Nonlinear vibration of imperfect eccentrically stiffened functionally graded double curved shallow shells resting on elastic foundation using the first order shear deformation theory", *Int. J. Mech. Sci.*, **80**, 16-28. https://doi.org/10.1016/j.ijmecsci.2013.12.009.

Kadum Njim, E., Al-Maamori, M.H., Madan, R., H Bakhy, S., Al-Waily, M., Khobragade, P. and Hadji, L. (2024), "Numerical and analytical investigation of free vibration behavior of porous functionally graded sandwich plates", *Mech. Adv. Compos. Struct.*, https://doi.org/10.22075/macs.2024.34962.1710.

Karamanlı, A. (2018), "Free vibration analysis of two directional functionally graded beams using a third order shear deformation theory", *Compos. Struct.*, **189**, 127-136. https://doi.org/10.1016/j.compstruct.2018.01.060.

Khayra, D., Meziane, M.A.A., Hadji, L., Atmane, H.A., Bennai, R. and Madan, R. (2024), "Effect of porosity and boundary conditions on dynamic characteristics of cracked plates made of functionally graded materials", *Adv. Concrete Constr.*, **18**(3), 175-190. https://doi.org/10.12989/acc.2024.18.3.175.

Kiarasi, F., Babaei, M., Asemi, K., Dimitri, R. and Tornabene, F. (2022), "Free vibration analysis of thick annular functionally graded plate integrated with piezo-magneto-electro-elastic layers in a hygrothermal environment", *Appl. Sci.*, **12**(20), 10682. https://doi.org/10.3390/app122010682.

Kumar, R., Miglani, A. and Kumar, R. (2024), "Axisymmetric deformation of thick circular plate in microelongated thermoelastic solid", *Couple. Syst. Mech.*, **13**(3), 231-245. https://doi.org/10.12989/csm.2024.13.3.231.

Li, S.R., Fu, X.H. and Batra, R.C. (2010), "Free vibration of three-layer circular cylindrical shells with functionally graded middle layer", *Mech. Res. Commun.*, **37**(6), 577-580. https://doi.org/10.1016/j.mechrescom.2010.07.006.

Madan, R. and Bhowmick, S. (2021), "A numerical solution to thermo-mechanical behavior of temperature dependent rotating functionally graded annulus disks", *Aircraft Eng. Aerosp. Technol.*, **93**(4), 733-744. https://doi.org/10.1108/AEAT-01-2021-0012.

Madan, R., Khobragade, P. and Bhowmick, S. (2024), "Impact of porosity on free vibration and limit analysis of power-law-based functionally graded disks", *Multidis. Model. Mater. Struct.*, **20**(6), 1192-1212. https://doi.org/10.1108/MMMS-04-2024-0108.

Matsunaga, H. (2008), "Free vibration and stability of functionally graded shallow shells according to a 2D higher-order deformation theory", *Compos. Struct.*, **84**(2), 132-146. https://doi.org/10.1016/j.compstruct.2007.07.006.

Mouthanna, A., Bakhy, S.H. and Al-Waily, M. (2023), "Analytical investigation of nonlinear free vibration of porous eccentrically stiffened functionally graded sandwich cylindrical shell panels", *Iran. J. Sci. Technol., Trans. Mech. Eng.*, **47**(3), 1035-1053. https://doi.org/10.1007/s40997-022-00555-4.

Mouthanna, A., Hasan, H.M. and Najim, K.B. (2018), "Nonlinear vibration analysis of functionally graded imperfection of cylindrical panels reinforced with different types of stiffeners", *2018 11th International Conference on Developments in eSystems Engineering (DeSE)*, 284-289.

Neamah, R.A., Nassar, A.A., Alansari, L.S., Njim, E.K. and Madan, R. (2025), "Experimental and analytical investigation of free vibration of a crack FG beam reinforced with alumina nano particles", *Adv. Nano Res.*, **18**(1), 19-31. https://doi.org/10.12989/anr.2025.18.1.019.

Njim, E.K., Hasan, H.R., Jweeg, M.J., Al-Waily, M., Hameed, A.A., Youssef, A.M. and Elsayed, F.M. (2024), "Mechanical properties of sandwiched construction with composite and hybrid core structure",

Adv. Polym. Technol., **2024**(1), 3803199. https://doi.org/10.1155/2024/3803199.

Njim, E.K., Jweeg, M.J., Al-Maamori, M.H., Idan, Z.S., Al-Waily, M., Mouthanna, A. and Hadji, L. (2024), "Wear Behavior analysis of imperfect functionally graded parts: Analytical and experimental techniques", *BIO Web Conf.*, **97**, 00001. https://doi.org/10.1051/bioconf/20249700001.

Quan, T.Q., Tran, P., Tuan, N.D. and Duc, N.D. (2015), "Nonlinear dynamic analysis and vibration of shear deformable eccentrically stiffened S-FGM cylindrical panels with metal-ceramic-metal layers resting on elastic foundations", *Compos. Struct.*, **126**, 16-33. https://doi.org/10.1016/j.compstruct.2015.02.056.

Raad, H., Najim, E., Jweeg, M., AlWaily, M., Hadji, L. and Madan, R. (2024), "Vibration analysis of sandwich plates with hybrid composite cores combining porous polymer and foam structures", *Journal of Comput. Appl. Mech.*, **55**(3), 485-499. https://doi.org/10.22059/jcamech.2024.377658.1121.

Rajawat, A.S., Sharma, A.K. and Gehlot, P. (2018), "Free vibration analysis of Stiffened Laminated Plate using FEM", *Mater. Today: Proce.*, **5**(2), 5313-5321. https://doi.org/10.1016/j.matpr.2017.12.115.

Singh, M., Saini, D.S., Matharu, S.P.S. and Salim, M. (2023), "Finite element analysis of alloy based hip implant under static loading conditions", *Recent Advances in Material, Manufacturing, and Machine Learning*, CRC Press.

Singh, S.K., Sondhi, L., Sahu, R.K., Madan, R. and Yadav, S. (2024), "Investigating thermo-mechanical stresses in functionally graded disks using Navier's method for different loading conditions", *Struct. Eng. Mech.*, **91**(6), 627-642. https://doi.org/10.12989/sem.2024.91.6.627.

Sofiyev, A.H. (2018), "Application of the first order shear deformation theory to the solution of free vibration problem for laminated conical shells", *Compos. Struct.*, **188**, 340-346. https://doi.org/10.1016/j.compstruct.2018.01.016.

Taheran, F., Monfared, V., Daneshmand, S. and Abedi, E. (2016), "Nonlinear vibration analysis of directional drill string considering effect of drilling mud and weight on bit", *J. Vibroeng.*, **18**(2), 1280-1287. https://doi.org/10.21595/jve.2015.16480.

Tayeb, B., Abderezak, R. and Daouadji, T.H. (2024), "Mechanical behavior of composite beam aluminum-sandwich honeycomb strengthened by imperfect FGM plate under thermo-mechanical loading", *Couple. Syst. Mech.*, **13**(2), 133-151. https://doi.org/10.12989/csm.2024.13.2.133.

Vini, M.H. and Daneshmand, S. (2019), "Investigation of bonding properties of Al/Cu bimetallic laminates fabricated by the asymmetric roll bonding techniques", *Adv. Comput. Des.*, **4**(1), 33-41. https://doi.org/10.12989/acd.2019.4.1.033.

Zohra, A., Rabia, B. and Tahar, H.D. (2024), "Study and analysis of porosity distribution effects on the buckling behavior of functionally graded plates subjected to diverse thermal loading", *Couple. Syst. Mech.*, **13**(2), 115-132. https://doi.org/10.12989/csm.2024.13.2.115.

Zouatnia, N., Hadji, L., Atmane, H.A., Nebab, M., Madan, R., Bennai, R. and Dahmane, M. (2024), "Analysis of free vibration in bi-directional power law-based FG beams employing RSD theory", *Couple. Syst. Mech.*, **13**(4), 359-373. https://doi.org/10.12989/csm.2024.13.4.359.

Nomenclature

a	: Panel length	(m)
b	: Span length	(m)
R	: Panel radius	(m)
H	: Panel thickness	(m)
C	: Ceramic	
M	: Metal	
Vc	: Volume fraction of ceramic	
Vm	: Volume fraction of metal	
Z_x, Z_y	: Eccentricities stiffened	(m)
S_x, S_y	: Distance between the transversal and longitudinal stiffeners	(m)
I_x, I_y	: Second moment of the cross-section areas for the stiffeners	(m^4)
u,v	: Displacement components along x, y	(m)
w	: The deflection of the panel	(m)
A_x, A_y	: Cross-section areas of the stiffeners	(m^2)
w_0, w^*	: Initial imperfection	(m)
K_s	: Shear correction factor	(m)
Q_x, Q_y	: The transverse force resultants	(Newton)

Appendix

$$A_{11} = \frac{1}{\Delta}\left(I_{10} + \frac{E_0 A_x}{s_x}\right), A_{22} = \frac{1}{\Delta}\left(I_{10} + \frac{E_0 A_y}{s_y}\right),$$

$$A_{12} = \frac{I_{20}}{\Delta}, A_{66} = \frac{1}{I_{30}},$$

$$\Delta = \left(I_{10} + \frac{E_0 A_x}{s_x}\right)\left(I_{10} + \frac{E_0 A_y}{s_y}\right) - I_{20}^2,$$

$$B_{11} = A_{22}(I_{11} + C_x) - A_{12} I_{21},$$

$$B_{22} = A_{11}(I_{11} + C_y) - A_{12} I_{21},$$

$$B_{12} = A_{22} I_{21} - A_{12}(I_{11} + C_y),$$

$$B_{21} = A_{11} I_{21} - A_{12}(I_{11} + C_x),$$

$$B_{66} = \frac{I_{31}}{I_{30}},$$

$$R_{22}(\phi_x) = D_{11}\frac{\partial^2 \phi_x}{\partial x^2} + D_{66}\frac{\partial^2 \phi_y}{\partial y^2} - K I_{30}\phi_x,$$

$$R_{23}(\phi_y) = (D_{12} + D_{66})\frac{\partial^2 \phi_y}{\partial x \partial y},$$

$$S_2(f) = B_{21}\frac{\partial^3 f}{\partial x^3} + (B_{11} - B_{66})\frac{\partial^3 f}{\partial x \partial y^2},$$

$$R_{31}(w) = -K I_{30}\frac{\partial w}{\partial y},$$

$$R_{32}(\phi_x) = (D_{21} + D_{66})\frac{\partial^2 \phi_x}{\partial x \partial y},$$

$$R_{33}(\phi_y) = D_{22}\frac{\partial^2 \phi_y}{\partial y^2} + D_{66}\frac{\partial^2 \phi_y}{\partial x^2} - KI_{30}\phi_y,$$

$$S_3(f) = B_{12}\frac{\partial^3 f}{\partial y^3} + (B_{22} - B_{66})\frac{\partial^3 f}{\partial x^2 \partial y},$$

$$a_1 = r_{11} + r_{12}\frac{r_{23}r_{31} - r_{21}r_{33}}{r_{22}r_{33} - r_{32}r_{23}} + r_{13}\frac{r_{32}r_{21} - r_{22}r_{31}}{r_{22}r_{33} - r_{32}r_{23}},$$

$$a_2 = r_{12}\frac{n_9 r_{23} - n_7 r_{33}}{r_{22}r_{33} - r_{32}r_{23}} + r_{13}\frac{n_7 r_{32} - n_9 r_{22}}{r_{22}r_{33} - r_{32}r_{23}} + r_{16},$$

$$a_3 = r_{14}\frac{r_{23}r_{31} - r_{21}r_{33}}{r_{22}r_{33} - r_{32}r_{23}} + r_{15}\frac{r_{32}r_{21} - r_{22}r_{31}}{r_{22}r_{33} - r_{32}r_{23}},$$

$$a_4 = r_{12}\frac{n_{10}r_{23} - n_8 r_{33}}{r_{22}r_{33} - r_{32}r_{23}} + r_{13}\frac{n_8 r_{32} - n_{10}r_{22}}{r_{22}r_{33} - r_{32}r_{23}},$$

$$a_5 = r_{14}\frac{n_{10}r_{23} - n_8 r_{33}}{r_{22}r_{33} - r_{32}r_{23}} + r_{15}\frac{n_8 r_{32} - n_{10}r_{22}}{r_{22}r_{33} - r_{32}r_{23}},$$

$$a_6 = r_{14}\frac{n_9 r_{23} - n_7 r_{33}}{r_{22}r_{33} - r_{32}r_{23}} + r_{15}\frac{n_7 r_{32} - n_9 r_{22}}{r_{22}r_{33} - r_{32}r_{23}},$$

$$r_{32} = -(D_{21} + D_{66})\lambda_m \delta_n - B_{12}\frac{\zeta}{S}\delta_n^3 - (B_{22} - B_{66})\frac{\zeta}{S}\lambda_m^2 \delta_n,$$

$$r_{33} = -D_{22}\delta_n^2 - D_{66}\lambda_m^2 - K_s I_{30} - B_{12}\frac{\Psi}{S}\delta_n^3 - (B_{22} - B_{66})\frac{\Psi}{S}\lambda_m^2 \delta_n,$$

$$n_9 = -K_s I_{30}\delta_n, n_{10} = -\frac{8}{3}\frac{B_{12}}{A_{22}}\frac{\lambda_m}{ab}, \zeta = B_{21}\lambda_m^3 + (B_{11} - B_{66})\lambda_m \delta_n^2,$$

$$\Psi = B_{12}\delta_n^3 + (B_{22} - B_{66})\lambda_m^2 \delta_n, S = A_{11}\lambda_m^4 + A_{22}\delta_n^4 + (A_{66} - 2A_{12})\lambda_m^2 \delta_n^2,$$

$$H_{19} = \frac{\delta_n^3 \lambda_m (\lambda_m^2 A_{12} + \delta_n^2 A_{22})}{8abH_{11}}, H_{21} = \frac{\lambda_m^3 \delta_n (\delta_n^2 A_{12} + \lambda_m^2 A_{11})}{4abH_{11}},$$

$$H_{22} = \frac{\lambda_m \delta_n^3 (\lambda_m^2 A_{12} + \delta_n^2 A_{22})}{4abH_{11}}, H_{23} = \frac{\lambda_m^2 (C_{11}^* A_{11} + C_{22}^* A_{12})}{H_{11}},$$

$$H_{24} = \frac{\delta_n^2 (C_{11}^* A_{12} + C_{22}^* A_{22})}{H_{11}}, H_{25} = \frac{8\lambda_m \delta_n}{ab},$$

$$D_{11} = I_{12} + \frac{E_0 I_x}{s_x} - B_{11}B_{12} - I_{21}B_{21},$$

$$D_{22} = I_{22} + \frac{E_0 I_y}{s_y} - B_{22}(I_{11} + C_y) - I_{21}B_{12},$$

$$D_{12} = I_{22} - B_{12}(I_{11} + C_x) - I_{21}B_{22},$$

$$D_{21} = I_{22} - B_{21}(I_{11} + C_y) - I_{21}B_{11},$$

$$D_{66} = I_{32} - I_{31}B_{66},$$

$$R_{11}(w) = KI_{30}\frac{\partial^2 w}{\partial x^2} + KI_{30}\frac{\partial^2 w}{\partial y^2} - k_1 w + k_2\left(\frac{\partial^2 w}{\partial x^2} + \frac{\partial^2 w}{\partial y^2}\right),$$

$$R_{12}(\phi_x) = KI_{30}\frac{\partial \phi_x}{\partial x},$$

$$R_{13}(\phi_y) = KI_{30}\frac{\partial \phi_y}{\partial y},$$

$$S_1(w,f)=\frac{\partial^2 f}{\partial x^2}\frac{\partial^2 w}{\partial x^2}-2\frac{\partial^2 f}{\partial x\partial y}\frac{\partial^2 w}{\partial x\partial y}+\frac{\partial^2 f}{\partial x^2}\frac{\partial^2 w}{\partial y^2}+\frac{1}{R}\frac{\partial^2 f}{\partial x^2},$$

$$R_{21}(w)=-KI_{30}\frac{\partial w}{\partial x},$$

$$H_{26}=A_{11}\lambda_m^4+A_{22}\delta_n^4+\left(A_{66}-2A_{12}\right)\lambda_m^2\delta_n^2, H_{27}=B_{21}\lambda_m^3+\left(B_{11}-B_{66}\right)$$

$$\lambda_m\delta_n^2, H_{28}=B_{12}\delta_n^3+\left(B_{22}-B_{66}\right)\lambda_m^2\delta_n, H_{29}=\frac{16\lambda_m^2\delta_n^2}{3mn\pi^2},$$

$$H_{31}=\frac{\delta_n^2}{3A_{11}mn\pi^2R}, H_{32}=\frac{16}{mn\pi^2}, \Phi_1=(\Delta T)(h)\amalg,$$

$$\amalg=\left(E_m\alpha_m+\frac{E_m(\alpha_c-\alpha_m)+\alpha_m(E_c-E_m)}{N+1}+\frac{(E_c-E_m)(\alpha_c-\alpha_m)}{2N+1}\right),$$

$$r_{11}=-\left(K_1+K_2\left(\lambda_m^2+\delta_n^2\right)+\frac{\lambda_m^4}{H_{26}R^2}\right), r_{12}=-\lambda_m^2\frac{H_{27}}{H_{26}R}-K_sI_{30}\lambda_m,$$

$$r_{13}=-\lambda_m^2\frac{H_{28}}{H_{26}R}-K_sI_{30}\delta_n, r_{14}=\left(H_{12}+H_{13}\right)-\frac{H_{25}H_{27}}{H_{26}}-\frac{H_{27}H_{29}}{H_{26}},$$

$$r_{15}=\left(H_{14}+H_{15}\right)-\frac{H_{25}H_{28}}{H_{26}}-\frac{H_{28}H_{29}}{H_{26}}, r_{16}=\left(H_{23}+H_{24}\right)\Phi_1-K_sI_{30}\lambda_m^2-K_sI_{30}\delta_n^2,$$

$$r_{17}=\left(H_{16}+H_{17}\right)-\frac{H_{25}\lambda_m^2}{H_{26}R}-\frac{H_{29}\lambda_m^2}{H_{26}R}-H_{31}, r_{18}=\left(H_{16}+H_{17}\right)-\frac{H_{25}\lambda_m^2}{H_{26}R}-\frac{H_{29}\lambda_m^2}{H_{26}R}-2H_{31},$$

$$r_{19}=-\left(H_{18}+H_{19}\right)-\frac{1}{16}\left(\frac{\lambda_m^2}{A_{22}}+\frac{\delta_n^2}{A_{11}}\right), r_{110}=-\left(H_{18}+H_{19}\right)-\left(H_{21}+H_{22}\right)-\frac{3}{16}\left(\frac{\lambda_m^4}{A_{22}}+\frac{\delta_n^4}{A_{11}}\right),$$

$$r_{111}=-\left(H_{21}+H_{22}\right)-\frac{1}{8}\left(\frac{\lambda_m^4}{A_{22}}+\frac{\delta_n^4}{A_{11}}\right), r_{21}=-B_{21}\frac{1}{S}\frac{\lambda_m^2}{R}\lambda_m^3-\left(B_{11}-B_{66}\right)\frac{1}{S}\frac{\lambda_m^2}{R}\lambda_m\delta_n^2,$$

$$r_{22}=-D_{11}\lambda_m^2-D_{66}\delta_n^2-K_sI_{30}-B_{21}\frac{\zeta}{S}\lambda_m^3-\left(B_{11}-B_{66}\right)\frac{\zeta}{S}\lambda_m\delta_n^2,$$

$$r_{23}=-\left(D_{12}+D_{66}\right)\lambda_m\delta_n-B_{21}\frac{\Psi}{S}\lambda_m^3-\left(B_{11}-B_{66}\right)\frac{\Psi}{S}\lambda_m\delta_n^2,$$

$$n_7=-K_sI_{30}\lambda_m, n_8=-\frac{8}{3}\frac{B_{21}}{A_{11}}\frac{\delta_n}{ab}, \tilde{\rho}_1=\left(\mathrm{I}_2-\frac{\mathrm{I}_1^2}{\mathrm{I}_0}\right),$$

$$r_{31}=-B_{12}\frac{1}{S}\frac{\lambda_m^2}{R}\delta_n^3-\left(B_{22}-B_{66}\right)\frac{1}{S}\frac{\lambda_m^2}{R}\delta_n\lambda_m^2,$$

$$C_{11}^*=\frac{1}{\Delta}\left(I_{20}-I_{10}-\frac{E_\circ A_x^T}{S_x^T}\right), C_{22}^*=\frac{1}{\Delta}\left(I_{20}-I_{10}-\frac{E_\circ A_y^T}{S_y^T}\right),$$

$$H_{11}=(A_{11}A_{22}-A_{12}^2), H_{12}=\frac{4\lambda_m^2(B_{21}A_{12}+A_{11}B_{11})}{\delta_n abH_{11}},$$

$$H_{13}=\frac{4\delta_n(B_{11}A_{12}+A_{11}A_{22}B_{21})}{abH_{11}}, H_{14}=\frac{4\lambda_m(B_{22}A_{12}+A_{11}B_{12})}{abH_{11}},$$

$$H_{15}=\frac{4\delta_n^2(B_{12}A_{12}+A_{22}B_{22})}{\lambda_m abH_{11}}, H_{16}=\frac{4\lambda_m A_{12}}{\delta_n RH_{11}},$$

$$H_{17}=\frac{4\delta_n A_{22}}{\lambda_m RH_{11}}, H_{18}=\frac{\lambda_m^3\delta_n(\delta_n^2A_{12}+\lambda_m^2A_{22})}{8abH_{11}},$$